ELSEVIER

ScienceDirect

Physics Procedia 2 (2009) 501–514

Physics Procedia

www.elsevier.com/locate/procedia

Synthesis and Thermoluminescence Properties of Mg^{2+} Doped Nanostructured Aluminium Oxide

J. F. S. Bitencourt[1] and S. H. Tatumi[1,2]

[1] Departamento de Engenharia Elétrica, Universidade de São Paulo, Luciano Gualberto Avenue, 380, 05508-900, Sao Paulo,SP – Brazil. jfsousab@yahoo.com.br

[2] Departamento de Ensino Geral , Faculdade de Tecnologia de São Paulo, Fernando Prestes Square, 30, 01124-060, Sao Paulo,SP – Brazil. tatumi@fatecsp.br

ABSTRACT

Samples of α-Al_2O_3: Mg were obtained using polymer calcination method, with five different concentrations of magnesium. ICP-AES analysis showed the magnesium concentrations to be: 0.47, 0.88, 1.33, 2.61 and 3.36 mol%. Scanning Electronic Microscopy (SEM) indicated the occurrence of a nanometric layer over the α-Al_2O_3 crystals surface and so did the Transmission Electronic Microscopy (TEM). The composition of this layer was found to be magnesium spinel ($MgAl_2O_4$) by Electron-beam diffraction, and according to the present results, it is related to the improvement of thermoluminescence (TL) emission efficiency, for γ-rays irradiated aliquots in the VIS and the near-UV regions. Theoretical deconvolution of experimental data using the Second Order Kinetics model originated into four TL emission peaks at 190, 280, 340 and 430ºC.

PACS: 78.60.Kn, 87.53.Bn, 29.40.-n, 78.67.-n, 78.67.Bf.

Keywords: Aluminium oxide, thermoluminescence properties, dosimetry, magnesium spinel, TEM, SEM.

INTRODUCTION

Study of thermoluminescence properties of aluminium oxide was suggested by Daniels' group in 1957 [1], but it was abandoned due to the preference to other more sensitive materials. Applications with aluminium oxide reappeared using samples doped with Mg and Y during the 1980's [2]. Since then, a large number of different compositions were created and theirs TL and Optical Stimulated Luminescence (OSL) properties have been investigated [3,4], in special using Al_2O_3:C.

It is known that alumina doped with Mg has luminescence and it related to the occurrence of F, F^+ and F^{++}-centers, i.e, anionic defects where electrons and holes recombine and emit light ([5], [6],[7], [8]).

During the crystal growth, oxygen vacancies are formed depending on the process conditions and parameters. The absence of one oxygen atom leaves behind a 2+ site. To maintain the crystal neutrality, this site can attract one electron, forming the F^+-center, or two electrons, forming the F-center. The F centers with divalent cations, as Mg^{2+}, substituting Al^{3+} on neighboring sites, can be stabilized more easily.

When the alumina is irradiated with high energy photons, electrons can be freed and trapped in unknown meta-stable states. If the alumina is heated TL can be emitted, obeying one of the cases below ([9], [6]):

$$F^+ + e^- \rightarrow F^* \rightarrow F + h\upsilon_{420nm} \quad (1)$$

$$F + h^+ \rightarrow F^{+*} \rightarrow F^+ + h\upsilon_{325nm} \quad (2)$$

$$F^{++} + e^- \rightarrow F^{+*} \rightarrow F^+ + h\upsilon_{329nm} \quad (3)$$

doi:10.1016/j.phpro.2009.07.036

In the equation (1) the F^+- center emission occur due to relaxation of F* from the ^3P to the $^3S^*$ level. Equation (2) represents the F^+ -center emission due to thermally released holes that recombine into to F centers, this results in excited F^+*-centers which relax from 2P to the 1S* level, it is cited in Li et al, 2007 [7] work that F^+-Mg centers have a high cross section for hole recombination, higher than that of isolated F^+-centers during electron irradiation. Finally, in the case of the equation (3), emission occurred due to recombination of thermally released electrons with F^{++} - centers, resulting in the F^{+*}- centers, relaxation of these ones from 1B to 1A level emit the 329nm photons.

MATERIALS AND METHODOLOGY

In the first step, five samples of fine powder α-alumina (<15 μm), doped with different concentration of magnesium, were prepared by polymer calcination method. ICP-AES (Inductively Coupled Plasma Atomic Emission Spectroscopy) analysis was used to determine Mg concentrations in the samples.

For Scanning Electronic Microscopy (SEM) analysis, model Nova 400 Nano SEM from FEI Company was used.

Transmission Electronic Microscopy (TEM) and Electronic Diffractometry (ED) were carried out using Philips CM200 and voltage around 160 keV.

For gamma-irradiation (^{60}Co), the samples were irradiated with the dose of 0.75 kGy, with rate around 237.5 Gy/h.

TL measurements were taken in TL/OSL equipment from Daybreak Nuclear and Medical Systems Inc., using optical filter Schott BG-39 (296 – 630 nm) for VIS and UV emissions, and Schott U-340 (267 – 377.5 nm) for UV emission. Heating rate of 5°C/s and preheating at 100°C for 10 s were set in the TL equipment. Each measured aliquot had around 1.8 mg for general TL.

RESULTS AND DISCUSSION

ICP-AES analysis demonstrated that the occurrence of magnesium in the five samples was: 0.44, 0.88, 1.33, 2.61 and 3.36 mol%. Hence, the structural and luminescent properties changes described below were due to the presence and concentration of magnesium atoms in the crystal lattice.

For doped samples, except the one with 3.36 mol% of magnesium, formation of thin layer on the surface of the crystals was reported (Figure 1). Undoped sample did not exhibit such layer.

The increasing concentration of magnesium atoms tends to minimize aggregate dimensions; size distribution histograms (Figure 2) were mounted for each doping concentration, and the average results are shown in Figure 3.

TEM image (Figure 4) showed the same layer and its width could be estimated around 30 nm. The composition of such layer obtained by ED indicates magnesium spinel ($MgAl_2O_4$).

Alumina aggregates by the coalescence of nanometric spherical single-crystals, forming a "neck" between them.

Formation of nanometric pores (nanopores) was also observed (Figure 4), but it seems to be disconnected from TL response, because even undoped samples show pores of the same size, approximately, and TL response from doped samples is, so far, a hundred times greater than from undoped sample. For some thermoluminescent materials, the occurrence of nanopores is critical for luminescence enhancement [10], since it increases anionic vacancies concentration [11].

TL emission curves in the visible and UV region are shown in the Figure 5 and Figure 6, respectively. Both samples were irradiated with the dose 500 Gy.

Using theoretical Second Order Kinetics [12] curves, described by the equation (4), experimental peaks were fitted, and their parameters were calculated.

$$I(T) = s' \cdot n_0^2 \cdot exp\left(-\frac{E}{k \cdot T}\right) \cdot \left[1 + n_0 \cdot \frac{s'}{\beta} \cdot \int_{T0}^{T} exp\left(-\frac{E}{k \cdot T'}\right) \cdot dT\right]^{-2} \quad (4)$$

Knowing that:

$$s' = \frac{s \cdot A_m}{N.A_n} \quad (5)$$

Where **s** is the frequency factor, $\mathbf{n_0}$ is the initial concentration of trapped electron in the band gap, **E** is the activation energy of a electron trap center, **k** is the Boltzmann constant, **T** is the absolute room temperature, **β** is the heating rate, $\mathbf{A_m}$ is the charge recombination probability, $\mathbf{A_n}$ is the retrapping probability and **N** is the total concentration of one kind of trapping center.

The equation (4) is required for each one of the emission peaks found in an experimental measurement. Thus, there are different values of **s'**, **E** and $\mathbf{n_0}$. The other values are constants for one measurement.

Some conclusions can be taken from the theoretical fitting. First, the peaks at 199, 280, 334 and 428ºC in the visible region and the peaks at 202, 280, 360 and 432ºC in the UV region are the same, respectively. Dislocations of emission peak temperatures can occur due to the precision of the equipment and its wavelength. Calculated values for **E**, **s** and **τ** parameters are shown in Table I.

Consequently, the peaks at 280, 350 and 430ºC (average of the mentioned temperatures) seems to be placed deeply in the UV band, meanwhile the peak at 200ºC is located, mostly, in the visible band. The relative intensities agree with this proposition:

in the UV band, the peak at 200ºC is 40% smaller, the peak at 280ºC increases 7 times, the peak at 350ºC increases 2.5 times and the peak at 430ºC is 3 times greater, comparing to the visible emission.

CONCLUSIONS

We can conclude that the luminescence response of the material is due to the presence of intrinsic and extrinsic defects, mostly F and F^+ centers generated by oxygen vacancies, which concentration is raised in the presence of magnesium atoms. These atoms interfere in the local charge of oxygen vacancies, stabilizing it. The major concentration of recombination centers may be related to the creation of F and F^+ defects in the crystals [13]. These defects are present even in the undoped samples, what explains the formation of 200ºC TL peak even in the absence of magnesium atoms. Nonetheless, the presence of the dopant allows the local charge to be stabilized easily when an oxygen atom is missing.

These defects are expected to be created in the interface α-alumina/spinel (α-Al_2O_3/$MgAl_2O_3$), because spinel itself and pure alumina did not show such emission.

The TL peaks are related to different recombination centers, due to the variation of intensities taken in the visible and UV band.

When one oxygen atom is dislocated from its site, the local charge is 2+, as said before, and when one magnesium atom replaces one aluminium atom, the local charge is 1-. So, two magnesium atoms replacing two aluminium atoms near one oxygen vacancy, neutralizes the local charge. Using the Kröger & Vicks notation:

$$Al_2O_3 + 2Mg^{2+} = (2Mg_{Al}^{2+} + V_{O'})^X \quad (6)$$

Mg^{2+}_{Al} are magnesium atoms located in aluminium (Al) sites and V_O is oxygen vacancies. The "X" index means the neutrality of the molecule.

These emission results confirm the values described by Brock [14], who detected light emission at 328 and 420 nm.

The TL emission peak at 200°C seems to be related to electron recombination in F-centers, because visible emission is the sum of $F^{++}\rightarrow F^+$ and $F^+\rightarrow F$ transitions. Meanwhile, UV emission is only the transition $F^+\rightarrow F$. On the other hand, the intensities of the emission peaks at 280, 350 and 430°C are greater in the UV region, proving that must be another type of recombination center besides the F-centers. Nonetheless, these centers remain unknown.

The achievement of the present research is TL emission peak at 280°C, which was not reported yet, and is generated by the presence of magnesium atoms, since undoped sample did not exhibited such emission. Another report to be made is about the

great enhancement of TL intensity of high temperature peaks. A higher temperature peak means stable signal storage, critical for applications mentioned before.

FUNDING

Conselho Nacional de Desenvolvimento Científico e Tecnológico (CNPq) and Fundação de Amparo à Pesquisa do Estado de São Paulo (FAPESP).

ACKNOWLEDGMENTS

We would like to thank CTR (Centro de Tecnologia das Radiações) from the Instituto de Pesquisas Energéticas e Nucleares (IPEN/CNEM – SP, Brazil).

REFERENCES

[1] J. F. Rieke, F. Daniels, J. Phys. Chem. 61, 629, 1957.
[2] M. Osvay, T. Biró. Aluminium oxide in TL dosimetry. Nuclear Instruments and Methods 175, 60-61, 1980.
[3] S.W.S Mckeever, M.Moscovitch, P. D. Towsend. Thermoluminescence dosimetry materials: properties and uses. Nuclear Technology Publishing, Ashford, 1995.
[4] S. W. S McKeever, M. W. Blair, E. Bulur, R. Gaza, R. Kalchgruber, D.M. Klein, E.G.Yukihara. Recent advances in dosimetry using the optically stimulated luminescence of Al_2O_3: C. Radiation Protection Dosimetry 109, 269-276, 2004.
[5] S. K. Mohapatra and F. A. Kröger. Defect structure of α-Al_2O_3 doped with magnesium. Journal of American Ceramic Society 60, 141-148, 1977.
[6] B. D. Evans, M. Stapelbrock. Phys. Rev. B. 18 (12) 7089, 1978.
[7] B. Li, T. Hinklin, R. Laine, S. Rand. Ultraviolet nanophosphors. Journal of Luminescence 122-123, 345-347, 2007.
[8] M. S. Akselrod, V. S. Kortov, D. J. Kravetsky, V. I. Gotlib. Highly sensitive thermoluminescent anion-defect alpha-Al_2O_3: C Single Crystal Detectors. Radiation Protection Dosimetry 33, 119-122, 1990.
[9] S.Vincellér, G. Molnár, A. Berkene-Krachai and P. Iacconi. Influence of thermal quenching on the thermostimulated processes in α-Al_2O_3. Role of F and F+ Centres. Radiation Protection Dosimetry 100, 79-82, 2002.
[10] W. M. Azevedo et al. Highly sensitive thermoluminescent carbon doped nanoporous aluminium oxide detectors. Radiation Protection Dosimetry 119, 201-205, 2006.
[11] D. D. Jayaseelan et al. Thermo-mechanical stability of porous-alumina: effects of sintering parameters. Science and Technology of Advanced Materials 5, 387-392, 2004.
[12] R. Chen and Y. Kirsh. Analysis of Thermally Stimulated Processes. Oxford, Pergamon Press, 1981.
[13] E. Papin et al. Influence of point defects on the thermoluminescence of alpha-Al_2O_3: application to dosimetry. Radiation Protection Dosimetry 84, 91-94, 1999.
[14] L. R. Brock et al. Color centers in magnesium doped polycrystalline alumina. Material Research Society Symposium Proceedings 667, 2001.

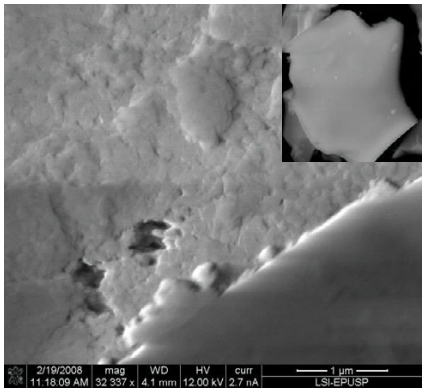
2/19/2008
11:18:09 AM
mag
32 337 x
WD
4.1 mm
HV
12.00 kV
curr
2.7 nA
1 µm
LSI-EPUSP

Figure 1

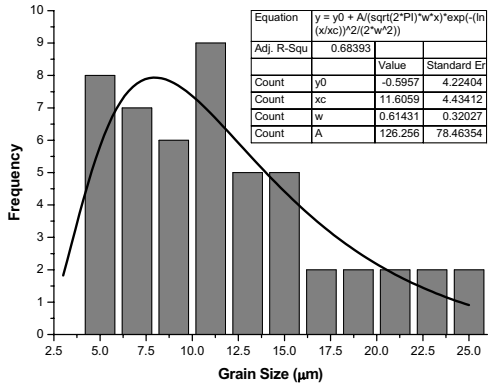
Equation
y = y0 + A/(sqrt(2*PI)*w*x)*exp(-(ln(x/xc))^2/(2*w^2))
Adj. R-Squ
0.68393
Value
Standard Er
Count
y0
-0.5957
4.22404
Count
xc
11.6059
4.43412
Count
w
0.61431
0.32027
Count
A
126.256
78.46354
Frequency
Grain Size (μm)
0
1
2
3
4
5
6
7
8
9
10
2.5
5.0
7.5
10.0
12.5
15.0
17.5
20.0
22.5
25.0

Figure 2

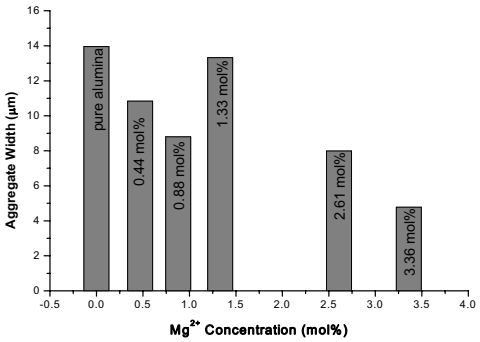
Aggregate Width (μm)
pure alumina
0.44 mol%
0.88 mol%
1.33 mol%
2.61 mol%
3.36 mol%
Mg2+ Concentration (mol%)

Figure 3

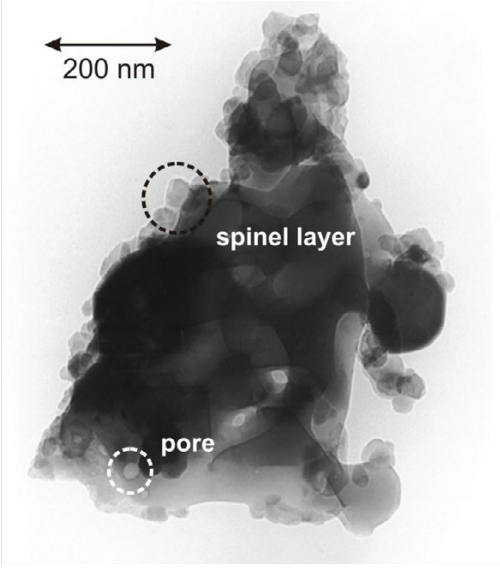

Figure 4

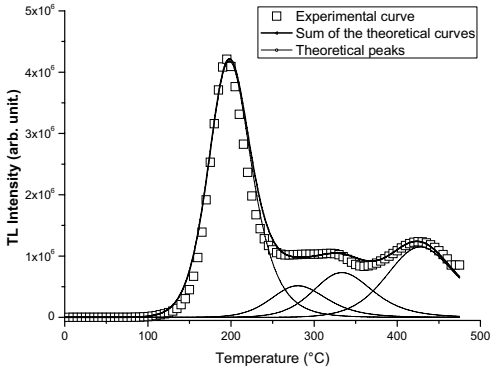
Experimental curve
Sum of the theoretical curves
Theoretical peaks
TL Intensity (arb. unit.)
5x10^6
4x10^6
3x10^6
2x10^6
1x10^6
0
0
100
200
300
400
500
Temperature (°C)

Figure 5

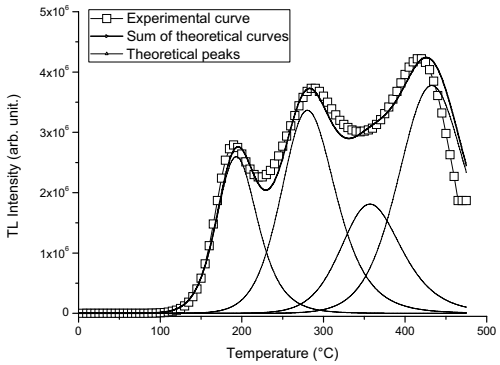
Experimental curve
Sum of theoretical curves
Theoretical peaks
TL Intensity (arb. unit.)
Temperature (°C)
5x10^6
4x10^6
3x10^6
2x10^6
1x10^6
0
0
100
200
300
400
500

Figure 6

Figures Captions

Figure 1. SEM image from sample Al_2O_3: Mg (2.61 mol%). A thin layer on the surface of the alumina crystal is shown; the surface was expected to be smooth for pure sample, just like the detail above.

Figure 2. Size distribution from grains produced by polymer calcination method. Average grain size is around 8 μm.

Figure 3. Variation of aggregate width in function of the Mg^{2+} concentration. A large concentration tends to shrink aggregate width.

Figure 4. TEM image from sample Al_2O_3: Mg (2.61 mol%). The thin layer observed in SEM image is shown with more details. The layer width is around 30 nm and composed by spinel crystallites. Pores formation is also observed.

Figure 5. TL emission curve from sample Al_2O_3: Mg (2.61 mol%) in the visible region. Second Order Kinetics curves were fitted to the experimental emission.

Figure 6. TL emission curve from sample Al_2O_3: Mg (2.61 mol%) in the UV region. Second Order Kinetics curves were fitted to the experimental emission.

Table I

T_m (°C)	E (eV)	s (s^{-1})	T (years)
185 – 202	1.0 – 1.04	$5.28x10^{10}$	0.037 – 0.176
280	1.1	$4x10^{9}$	23.583
337 – 360	1.23 – 1.28	$6x10^{9}$	2400 - 16600
428 – 435	1.39 – 1.4	$6x10^{9}$	$(2.33 – 3.43)x10^{6}$

Table Caption

Table I. Calculated parameters **E**, **s** and **τ** for each TL peak using Second Order Kinetics. Variation of the values were due to the deviation of TL peak for visible and UV emission.